AD-A256 879

②

RL-TR-92-87
In-House Report
July 1992

THE COMPONENTS OF AN OPTICAL RS FLIP-FLOP FOR AN INTEGRATED OPTICAL PROCESSOR

Dr. Michael A. Parker, Stuart I. Libby, 1/Lt, USAF,
Dr. Paul D. Swanson

DTIC
ELECTE
NOV 05 1992
E
D

92-28920

Rome Laboratory
Air Force Systems Command
Griffiss Air Force Base, NY 13441-5700

92 11 04 068

This report has been reviewed by the Rome Laboratory Public Affairs Office (PA) and is releasable to the National Technical Information Service (NTIS). At NTIS it will be releasable to the general public, including foreign nations.

RL-TR-92-87 has been reviewed and is approved for publication.

APPROVED:
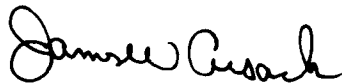
JAMES W. CUSACK, Chief
Photonics & Optics Division

FOR THE COMMANDER:

JAMES W. YOUNGBERG, LtCol, USAF
Deputy Director
Surveillance & Photonics Directorate

REPORT DOCUMENTATION PAGE

Public reporting burden for this collection of information is estimated to average 1 hour per response, including the time for reviewing instructions, searching existing data sources, gathering and maintaining the data needed, and completing and reviewing the collection of information. Send comments regarding this burden estimate or any other aspect of this collection of information, including suggestions for reducing this burden, to Washington Headquarters Services, Directorate for Information Operations and Reports, 1215 Jefferson Davis Highway, Suite 1204, Arlington, VA 22202-4302, and to the Office of Management and Budget, Paperwork Reduction Project (0704-0188), Washington, DC 20503.

1. AGENCY USE ONLY (Leave Blank)	2. REPORT DATE July 1992	3. REPORT TYPE AND DATES COVERED In-House Sep 90 – Jan 92

4. TITLE AND SUBTITLE THE COMPONENTS OF AN OPTICAL RS FLIP-FLOP FOR AN INTEGRATED OPTICAL PROCESSOR	5. FUNDING NUMBERS PE - 61101F PR - LDFP TA - 05 WU - H1
6. AUTHOR(S) Dr. Michael A. Parker, Stuart I. Libby, 1/Lt, USAF, Dr. Paul D. Swanson	

7. PERFORMING ORGANIZATION NAME(S) AND ADDRESS(ES)
Rome Laboratory (OCPB)   Cornell University
Griffiss AFB NY 13441-5700   Dept of Elec Engr
                             212 Phillips Hall
                             Ithaca NY 14853
	8. PERFORMING ORGANIZATION REPORT NUMBER
	RL-TR-92-87

9. SPONSORING/MONITORING AGENCY NAME(S) AND ADDRESS(ES) Rome Laboratory (OCPB) Griffiss AFB NY 13441-5700	10. SPONSORING/MONITORING AGENCY REPORT NUMBER

11. SUPPLEMENTARY NOTES

Rome Laboratory Project Engineer: Dr. Michael A. Parker/OCPB (315) 330-7671

12a. DISTRIBUTION/AVAILABILITY STATEMENT Approved for public release; distribution unlimited.	12b. DISTRIBUTION CODE

13. ABSTRACT (Maximum 200 words)

This report discusses the design, fabrication and test of an optical RS Flip-Flop as an integrated optical memory element. The Flip-Flop has three GaAs-AlGaAs heterostructure lasers with total internal reflection mirrors. A main laser incorporates a saturable absorber to develop the bistable output characteristics. A pump laser bleaches the absorber to set the logic 1 state. A third laser quenches the main laser to reset the device to logic 0. Experiments and data for the laser quenching and bistability are presented.

14. SUBJECT TERMS optical computing, optical logic, integrated circuit, optical flip flop	15. NUMBER OF PAGES 24
	16. PRICE CODE

17. SECURITY CLASSIFICATION OF REPORT UNCLASSIFIED	18. SECURITY CLASSIFICATION OF THIS PAGE UNCLASSIFIED	19. SECURITY CLASSIFICATION OF ABSTRACT UNCLASSIFIED	20. LIMITATION OF ABSTRACT U/L

ABSTRACT

We discuss the design, fabrication and test of an optical RS Flip-Flop as an integrated optical memory element. The Flip-Flop has three GaAs-AlGaAs heterostructure lasers with total internal reflection mirrors. A main laser incorporates a saturable absorber to develop the bistable output characteristics. A pump laser bleaches the absorber to set the logic 1 state. A third laser quenches the main laser to reset the device to logic 0. Experiments and data for the laser quenching and bistability are presented.

ACKNOWLEDGEMENTS

TABLE OF CONTENTS

I. INTRODUCTION

Considerable effort has been invested in the development of optical logic gates and memory elements for the realization of an integrated optical computer.[1] High laser threshold currents and the lack of integration techniques limited the usefulness of early designs for logic gates and memory elements based on semiconductor lasers. Recent developments in the epitaxial growth techniques for quantum well heterostructures and the processing techniques have since made the early designs attractive for optical computing purposes.

An optical RS flip-flop has been designed to function as an optical memory element. The flip-flop can be divided into 3 functional blocks (refer to figure 1). (1) A main laser cavity contains *gain* and *saturable absorber* sections[2-5] which induce bistable output characteristics; this functional block provides the logical 0 or 1 state. (2) An external laser *pumps* the saturable absorber and *sets* the output to the logic 1. (3) A second external laser quenches[6,7] the main laser and *resets* the output to the logic 0. These lasers are monolithically integrated on AlGaAs-GaAs quantum well heterostructure and they emit at 860 nM. The main cavity has one Total Internal Reflection (TIR) mirror[7] and a flat etched mirror which separates it from the pump laser. Reflections can occur at the discontinuity in the index of refraction accompanying the electrical isolation between the pumped and unpumped regions; thus the cut across the electrode is angled to inhibit the formation of a shorter cavity within the main cavity. The quench laser is divided into two parts across the gain region of the main laser[7] so that the quench and main laser cavities overlap; the two halves of the quench laser are electrically connected in parallel. All four gain sections have ridge waveguides but the voltage controlled saturable absorber is unguided when it is reverse biased.

The operation of the flip-flop depends on the ability of the pump and quench laser to set and reset the output state of the main cavity respectively. Figure 1 shows a qualitative plot of the intensity of the light emitted from the main laser versus the current into the gain section. The current in the main laser gain section is adjusted to point *M* where the output intensity can be in either of two states. Assume that initially the output of the main laser corresponds to a point on the lower branch of the hysteresis loop. A momentary optical pulse from the pump laser bleaches the absorber, lowers the threshold current below point *M* and, therefore, sets the output to the upper branch of the hysteresis loop. The bistable nature of the gain-absorber pair ensures that the output will remain on the upper branch for times longer than the width of the pulse. When a momentary optical pulse from the quench laser stimulates emission in the

1

common cavity, the wavevector of this stimulated emission is parallel to the cavity of the quench laser instead of the main laser.   This process reduces gain in the main cavity, raises the lasing threshold current and, thereby, resets the output of the main laser to the lower branch of the hysteresis curve.
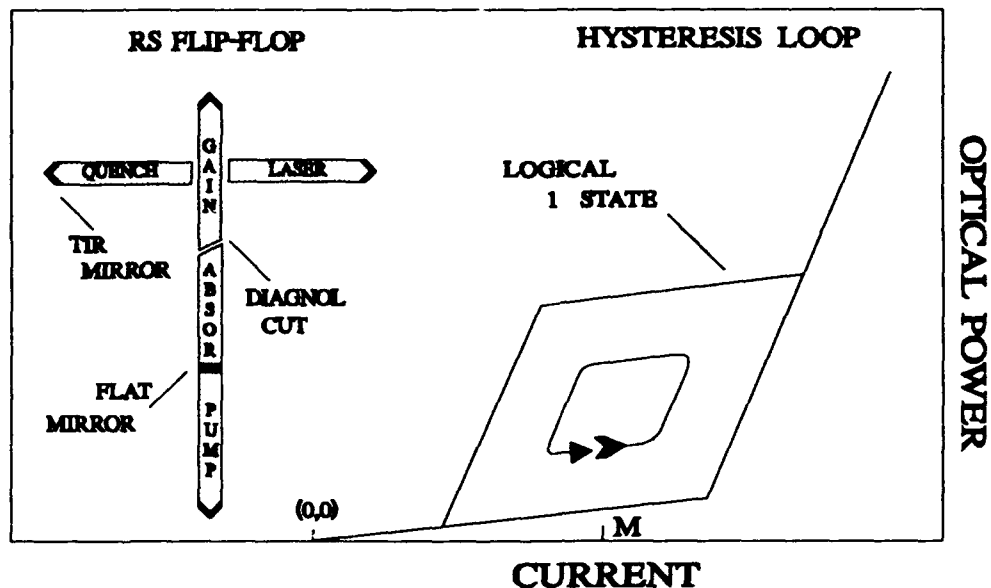

Figure 1:   The RS Flip-Flop and the hysteresis in the L-I characteristics.

Two of the three functional blocks of the RS flip-flop were fabricated and tested.   Optical NOR gates were fabricated to test the effects of quenching.   Gain - absorber pairs were constructed to test for the hysteresis effects. The NOR gates had ridge waveguides and mirrors which were etched in a *Chemically Assisted Ion Beam Etcher* (CAIBE).   The gain - absorber pairs had gain guided lasers, unguided saturable absorbers and cleaved mirrors; these devices were constructed with a variety of lengths for the gain and absorber sections.   Both quenching and hysteresis were observed.

The remainder of this report is divided into three sections: fabrication, experimental and discussion. The Fabrication section briefly describes the fabrication process.[10] The Experimental section contains a brief discussion of the experimental apparatus[11] and the results of the experiments. This section includes emitted light vs. current (L-I) characteristics, quenching data and hysteresis graphs.   The Discussion section contains the authors' interpretation of the data.
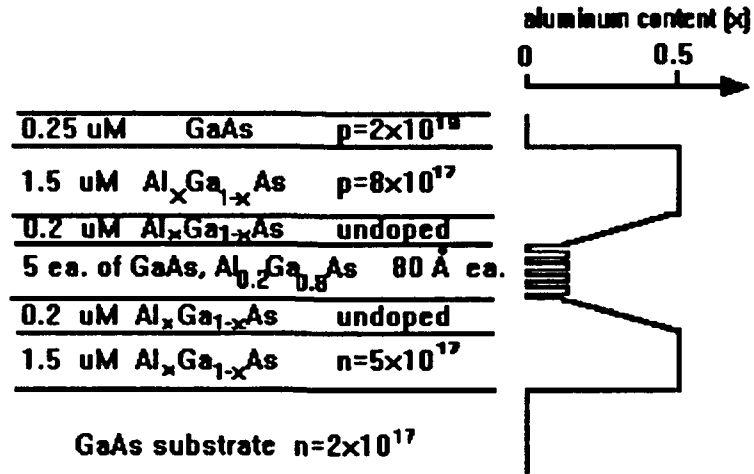
2

aluminum content (x)

0   0.5

0.25 uM	GaAs	p=2×10¹⁸
1.5 uM	Al$_x$Ga$_{1-x}$As	p=8×10¹⁷
0.2 uM	Al$_x$Ga$_{1-x}$As	undoped
5 ea. of GaAs, Al$_{0.2}$Ga$_{0.8}$As	80 Å ea.	
0.2 uM	Al$_x$Ga$_{1-x}$As	undoped
1.5 uM	Al$_x$Ga$_{1-x}$As	n=5×10¹⁷

GaAs substrate n=2×10¹⁷

Figure 2: The epitaxial layer structure of the multiquantum well wafer used for the RS flip-flop.

II. FABRICATION

All of the devices were fabricated from GaAs-AlGaAs quantum well wafers as shown in figure 2. The NOR gates and gain-absorber pairs fabricated (refer to figure 3) had CAIBE etched mirrors and ridge waveguides[8]. The main laser was 13 x 85 μm long and the quench lasers were about 20 x 200 μm. A shallow etch of 2 μm wide and 1.75 μm deep into the P$^+$ GaAs, shown in the expanded cross sectional view of figure 3, provided up to 1KΩ of electrical isolation between the top pads for the lasers. The mirrors[10] were formed by deep etches of 4.5 μm; residues on the wafer surface led to narrow spikes[9] in the GaAs substrate but they did not affect the quality of the mirror. An SiO$_2$ layer was used as electrical isolation as well as an etch retardation mask for the shallow etch process.[10] Large metal pads (not shown) were connected to the devices to supply the external bias; a layer of SiO$_2$, 1300 angstroms thick, electrically isolated the pad from the GaAs. The top P$^+$ Ohmic contacts[10,12] were made by diffusing zinc through openings in this SiO$_2$ layer to the depth of 0.3 μm, evaporating Ti, Pt, Au over the surface, using a liftoff process to remove regions of unwanted metal. The bottom N⁻ contact was made by depositing layers cf Ge, Ni, Ag and Au after lapping the bottom of the wafer so that the total wafer thickness was about 150 μm. Both the P and N Ohmic contacts were simultaneously annealed prior to cleaving out and testing the devices.

The gain-absorber pairs were fabricated with gain-guided gain sections and unguided, voltage controlled saturable absorbers. The processing steps were the same excluding the dry etching used to delineate the waveguides and mirrors. The structure appears in figure 3. The lengths in microns of the saturable absorber and gain sections are given by $L_a = 150 + 50n$ and $L_g = 350 - 50n$ for the integers n ε [0,3]. These devices had 10 μm wide, multimode waveguides.

3

NOR GATE
RIDGE WAVEGUIDES
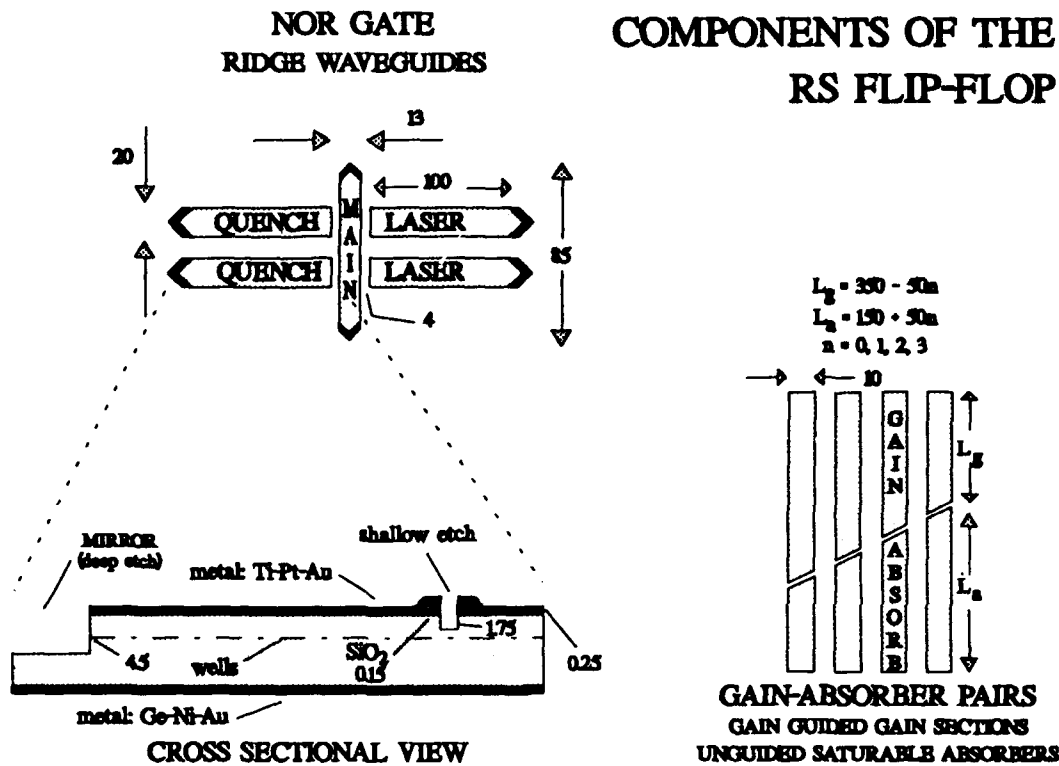
COMPONENTS OF THE
RS FLIP-FLOP

Figure 3: The components of the RS flip-flop. Laser quenching was tested with the NOR gates. The cross sectional view shows the layers and the etch depths for the NOR gate. The gain absorber pairs had gain- guided gain sections and unguided saturable absorbers.

III. EXPERIMENTAL

This section presents the experiments performed on the functional blocks of the RS Flip-Flop[12]. The first subsection contains the experimental setup and results for the quenching experiments and the associated L-I curves. The next subsection contains the saturable absorber experimental setup and results.

A. QUENCH EXPERIMENTS

L-I curves of the main laser in the NOR gates were taken in order to determine threshold currents and relative mirror reflectivity. TIR mirrors were designed into the RS flip-flops and used in the NOR gates in an attempt to reduce the threshold currents. In principle, the reflectivity of a TIR mirror can approach 100%; however, the actual reflectivity varies with processing due to lithographically limited rounding of the curves.

The experimental setup for obtaining the L-I curves appears in the inset to figure 4. The pulse generator produced 5 μsec wide pulses separated by 2 msec. The pulse itself was the positive portion of a sine wave. It was applied to the series combination of the main laser and a 50 Ω current sampling resistor which were joined at the bottom N⁻ contact. This resistor yielded a voltage drop proportional to the current through the laser. A single mode fiber, with one end positioned next to a facet of the main laser, routed the illumination to a PIN photodiode circuit. A digital oscilloscope plotted the pin diode signal versus the signal across the 50 Ω resistor.
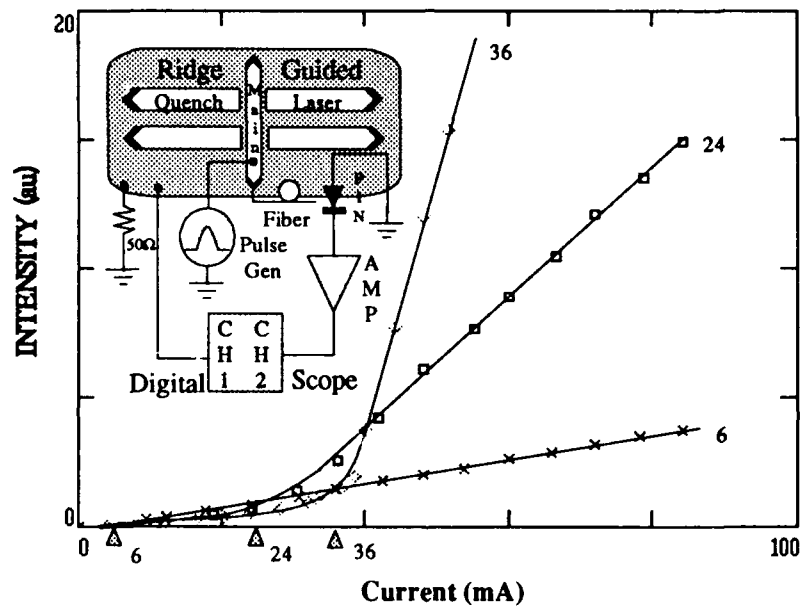

Figure 4: The L-I curves from main lasers with TIR mirrors in three different NOR gates. The numbers next to the triangles indicate the threshold currents. The inset shows the device and the experimental arrangement.

The L-I curves for three different main lasers with TIR mirrors and etched ridge waveguides appear in figure 4. Thresholds of 6, 24, and 36 mA were observed. The variation in threshold currents stems from the variation in processing across the surface of the wafer; the lasers with the lower threshold currents most probably had the better mirrors. It was conjectured that rounding at the tip of the mirror increased the light transmitted through the mirror, thus increasing the required threshold current.

The quench experiments[12] were conducted with the apparatus depicted by the block diagram in the inset to figure 5. A pulse generator applied a voltage to the main laser for about 10 microseconds.

5

During this time, a second synchronized pulse generator drove the side laser with a triangular wave of the same duration as the pulse in the main laser. One end of an optical fiber probed the emitted light. A pin photodiode and amplifier detected and amplified the optical signal and then applied the resulting signal to the digital oscilloscope. The currents through the main and side lasers were determined by monitoring the voltage across 10 Ω resistors in series with the pulse generators (not shown).
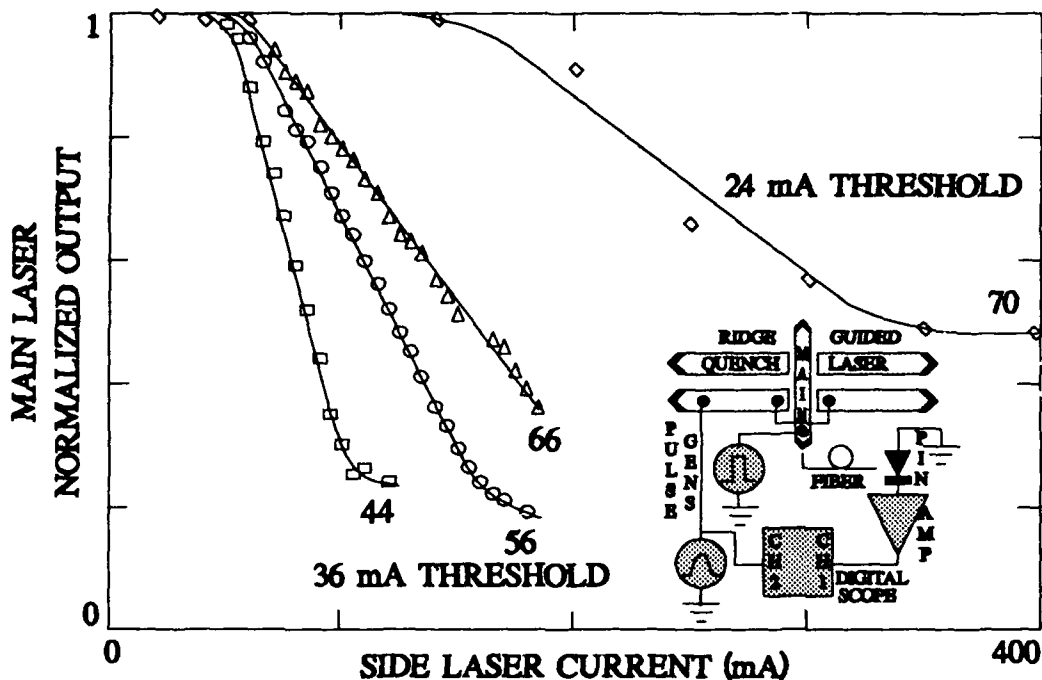

Figure 5:   Normalized irradiance from the main lasers of two NOR gates as a function of the current into the side lasers; threshold currents of 36 and 24 mA were determined from figure 4 for these lasers.   The quenching effect was observed for the 36 mA NOR gate with 44, 56 and 66 mA into the main laser and for the 24 mA NOR gate with 70 mA into the main laser.

Of the NOR gates tested, the results from two with differing threshold currents for the main laser appear in figure 5.   The graph plots the emitted power from the main laser as a function of the current injected into the side laser; the power has been normalized to unity.   The set of three curves correspond to the device with the 36 mA threshold current for the main laser while the right most curve corresponds to the device with the 24 mA threshold current.   The irradiance from the 6 mA device was too small for accurate measurements.   The values of the current injected into the main laser parameterize the curves. Approximately 80% of the optical power from the main laser can be quenched.   Note the fairly linear decrease in main laser intensity   as the side laser current increases.   Also note that more side laser current is required for larger main laser currents in order to maintain a constant amount of quench.   The gate with the 24 mA threshold for the main laser required larger quench currents than the gate with the 36 mA threshold for the main laser; in addition, this main laser could be quenched by no more than 50%.

6

The quenching can not be attributed to electrical crosstalk between the metal pads on the P$^+$ side of the wafer. Both the main and side lasers must be electrically biased in the same way. Therefore, electrical crosstalk would cause the current in one laser to increase as the current in the others increase. In this case, the power emitted from both must increase. Any resistance in the N$^-$ layer or in the circuit connecting the metal on the N$^-$ layer could give rise to curves which resemble the quench curves of figure 5. But, based on the doping level, the thickness of the N$^-$ layer,[13] and the device sizes, the typical resistance in this layer is on the order of 0.1 Ω. Any voltage drop across this resistance would be relatively small and could not account for the quench data.

B. SATURABLE ABSORBER EXPERIMENTS

The saturable absorber plays the key role in the RS flip-flop. It must induce the hysteresis loop shown in figure 1 and it must be capable of being bleached by illumination from a secondary laser in such a way that the main cavity begins to lase from an initially off state. The saturable absorber experiments include tests for (1) the hysteresis induced in the L-I curve of the main laser and (2) the width of the hysteresis loop as a function of the applied voltage.

In one series of experiments, ridge guided gain-absorber pairs were tested for hysteresis in the L-I characteristics. These pairs included those with (1) wet and CAIBE etched waveguides, (2) various lengths of gain and saturable absorber sections and (3) single and multi-mode waveguides. Hysteresis was not observed in any of the ridge guided devices. In another series of experiments, hysteresis was observed in devices with gain guided gain sections and unguided saturable absorbers; these devices are depicted in figure 3.

Intensity-Voltage curves (L-V) were determined for the gain and saturable absorber sections. Hysteresis was observed at peak current levels approaching 400 mA in the gain section. The experimental setup appears in the inset to figure 6. A pulse from a function generator was amplified and applied to the gain section of the laser cavity. The pulse consisted of the positive half of a sine wave and was generally 15 μs long with 2 n.s between pulses. The saturable absorber was reverse biased by a DC supply. The current injected into the gain section was determined by monitoring the voltage developed across a 10 Ω resistor placed in series with that section. One end of a single mode fiber probed the optical emission from the saturable absorber; the other end applied the optical signal to a PIN diode. The drive voltage and PIN signals were viewed on a dual trace digital oscilloscope as ch 1 vs. ch 2.
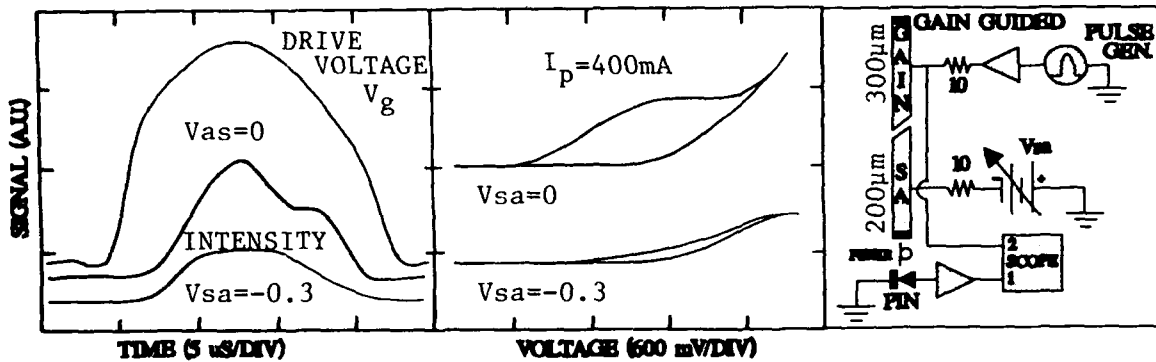
Figure 6: The left side shows plots of the timing relation between the drive voltage to the gain section of the gain-absorber pairs and the emitted irradiance from the pair; the irradiance is shown for two voltages on the saturable absorber. The middle panel shows the hysteresis loop for the emitted irradiance vs. drive voltage. The experimental setup is shown on the right.

The results for a typical device appear in figure 6. The vertical axis has arbitrary units in either voltage or irradiance. The left side of the plot shows the timing relation between the drive voltage to the gain section and the irradiance emitted through the saturable absorber. The hysteresis curves on the right hand side are plots of the irradiance vs. the drive voltage. The two intensity plots correspond to two different voltages applied to the saturable absorber. The slight asymmetry of the drive voltage results from the I-V and L-I characteristics of the laser diode as can be seen by comparing the drive voltage curve to the intensity curves.

Of particular interest is the hump on the right side of the $V_{sa}= 0$ intensity plot. Once the saturable absorber is bleached, it remains in that state for values of current into the gain section which are less than the initial threshold current. It is this hump which produces the upper hysteresis loop in figure 6. An increase of the reverse bias voltage causes the irradiance, the width and height of the loop to decrease. The loops can not be attributed to heating effects as the system would transverse the loop in a clockwise direction rather than the counter clockwise direction observed for these loops. No attempt was made to correct for RC effects present which probably dominated beyond about -0.6 volts; these effects can not explain the loops[11] for saturable absorber voltages less than about -0.6 volts. The Vsa= -1 volt loop appears to be mostly a result of RC effects. We did note that the position of the single mode fiber strongly influenced the shape of the observed L-I curves. We attributed this behavior to the occurrence of bistability for only certain modes present in the multimode structure.

The bistable characteristics were further investigated. The width of the loop was plotted as a function of the voltage applied to the saturable absorber as shown in figure 7. The width of the loop changed by an order of magnitude for a 1.4 volt change in the voltage applied to the saturable absorber. RC effects were probably responsible for the non-linear portion of the curve beyond about -0.6 volts.
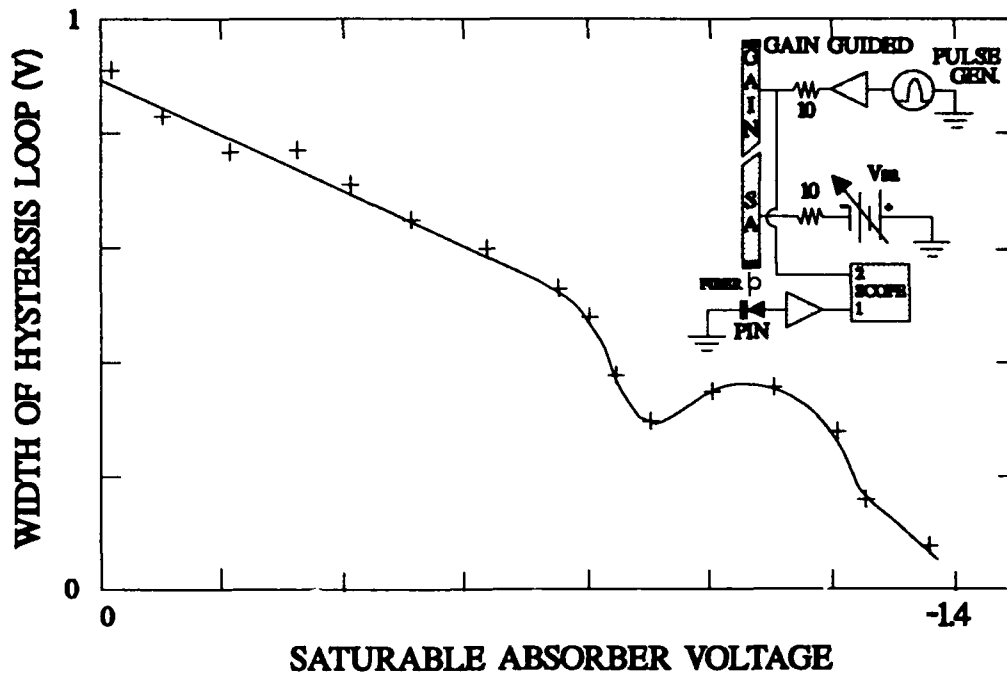
8

Figure 7: The width of the hysteresis loop as a function of the voltage applied to the saturable absorber. The effects of RC time delays have not been removed from the data which probably dominate the other effects in determining the width of the observed loops beyond about -0.6 volts. The inset shows the experimental setup used to observe the hysteresis loop.

IV DISCUSSION

The lasers with TIR mirrors have lower threshold currents but also lower differential efficiency (dL/dt for I above threshold) than similar lasers with flat etched mirrors. Optical losses such as scattering in the cavity, diffraction and mirror transmittance determine the differential efficiency and the threshold current.[14] The differential efficiency and threshold current decrease as the quality of the mirrors increases.

The quench curves in figure 5 consists of the Spontaneous Emission Region, the Linear Region and the Saturation Region. The Spontaneous Emission Region corresponds to side laser currents smaller than about 50 mA; this region is due to the lack of stimulated emission in the quench lasers. The irradiance from the main laser can increase to values larger than 1 if (i) the leakage current between the main and

quench lasers, which is through the unetched portion of the P^+ GaAs, is sufficiently large or if (ii) the spontaneous emission from the quench laser aids the pumping of the main cavity. LR refers to that part of the graph where the irradiance from the main laser linearly decreases. For this region, a photon from either the quench or main laser cavity can stimulate the emission of a photon from electron-hole recombination in such a way that the wave vector of this emission is parallel to either the quench or main laser cavity respectively.[13] However, above threshold, the photon density in the quench laser is linearly proportional to the quench laser pump current. Thus the probability of interaction between the photons from the quench laser and electron-hole pairs in the common cavity increases linearly. As a result, the gain of the main laser linearly decreases to a fixed value. Main lasers operating at higher current densities require larger quench laser currents to achieve the same amount of quench. The SR, the region where the irradiance saturates, occurs for relatively large values of the quench current. For small common cavity volumes, the main laser can not be quenched and intensity of the stimulated emission corresponds to the observed saturation level. For volumes of the common cavity sufficiently large to quench the main laser, the observed saturation level is due to the spontaneous emission from the main laser. At present, we can not explain the larger currents required to quench the lasers with the better mirrors.

Hysteresis in the L-I characteristics of the gain-absorber pair can be attributed to the characteristics of the saturable absorber. Below laser threshold, the saturable absorber presents a loss to the cavity which sets the threshold current at J_1 (for example). For currents just above J_1, the photon density abruptly jumps to the upper branch of the hysteresis loop. Once the output state of the device corresponds to a point on the upper branch, the current can be decreased to values somewhat smaller than J_1 without significantly affecting the emitted flux because, on the upper branch, the saturable absorber is still bleached for currents near J_1. At some current $J_2 < J_1$, the emitted flux will suddenly transition to the lower branch.

The hysteresis loops present in this paper are believed to be due to the mechanism described above. In this case, the voltage dependence of the loop width c be attributed to the quantum confined stark effect. The fact that the hysteresis was not observed for saturable absorbers with ridge waveguiding might be due to relatively low intensities necessary to saturate the absorption. The unguided saturable absorber sections would be less likely to mask the effect because the intensity of the light in the saturable absorber would be smaller due to diffraction effects. Another possibility consists of the self focusing of the light in the saturable absorber due to spatial hole burning.[15]

V SUMMARY

An optical RS flip-flop has been designed and presented for use as an optical memory element in an integrated optical processor. The design incorporated TIR mirrors, a main cavity with a gain section and a voltage controlled saturable absorber, a quench laser and a pump laser. Experiments tested for hysteresis in the L-I characteristics of ridge guided single and multi-mode waveguides with negative results. Hysteresis was found in gain-absorber pairs which had no waveguiding in the saturable absorber. The laser quenching was tested in logic gates with coupled cavities and TIR mirrors. The effect of the pump laser on the output state of the devices which exhibited hysteresis was not tested.

The final version of the optical RS flip-flop will employ a silicon diffusion process to delineate the waveguides and provide electrical isolation rather than the shallow etches presently used. The electrical isolation between the devices should increase to about 1 MΩ from the present value of 300 to 1000 Ω. The poor electrical isolation makes it difficult at times to distinguish between the optical and electrical effects. The use of this silicon diffusion process should dramatically improve the situation. The hysteresis and quenching obtained from these new devices will be modelled and then simulated on a computer.

REFERENCES

1. D. G. Feitelson, *Optical Computing*, MIT Press, Cambridge (1988)
2. G. J. Lasher, Solid-State Electronics, 7, 707 (1964)
3. T. Odagawa and S. Yamakashi, Electronics Letters, 25, 1429 (1989)
4. T. Ueno and R. Lang, J. Appl. Phys. 58, 1689 (1985)
5. C. Harder, K. Y. Lau, A. Yariv, IEEE J. Quant. Elect. QE-18, 1351 (1982)
6. W. J. Grande and C. L. Tang, Appl. Phys. Lett. 51, 1780 (1987)
7. W. Jung and Y. Kwon, Jap. J. Appl. Phys. 28, L1242 (1989)
8. W. J. Grande, W. D. Braddock, J. R. Sheally, C. L. Tang, Appl. Phys. Lett. 51, 2189 (1987)
9. W. J. Grande, J. E. Johnson, C. L. Tang, J. Vac. Sci. Technol. B8, 1075 (1990)
10. P. D. Swanson, S. Libby, M. A. Parker, *TheFabrication of Ridge Waveguided Photonic Circuits with Chemically Assisted Ion Beam Etched Mirrors*. USAF Technical Report, 1992 (in preparation).
11. S. L. Libby, P. D. Swanson, M. A. Parker, *Optical Logic Gate and Component Analysis Techniques*, USAF Technical Report, 1992 (in preparation).
12. M. A. Parker, A. Olewicz, S. I. Libby, D. Honey, P. D. Swanson, P^+ *Contacts on GaAs for Semiconductor Lasers*, USAF Technical Report (1992)
13. S. M. Sze, *Physics of Semiconductor Devices*, 2nd edition, John Wiley and Sons Inc., New York (1981).
14. M. A. Parker, P. D. Swanson, S. I. Libby, *The Importance of Optical Loss for the Differential Efficiency and Threshold Current in Quantum Well Lasers*, Rome Laboratory Technical Memorandum 1992 (in preparation).
15. R. Lang, J. J. Appl. Phys. 19, L93 (1980)

MISSION

OF

ROME LABORATORY

Rome Laboratory plans and executes an interdisciplinary program in research, development, test, and technology transition in support of Air Force Command, Control, Communications and Intelligence (C^3I) activities for all Air Force platforms. It also executes selected acquisition programs in several areas of expertise. Technical and engineering support within areas of competence is provided to ESD Program Offices (POs) and other ESD elements to perform effective acquisition of C^3I systems. In addition, Rome Laboratory's technology supports other AFSC Product Divisions, the Air Force user community, and other DOD and non-DOD agencies. Rome Laboratory maintains technical competence and research programs in areas including, but not limited to, communications, command and control, battle management, intelligence information processing, computational sciences and software producibility, wide area surveillance/sensors, signal processing, solid state sciences, photonics, electromagnetic technology, superconductivity, and electronic reliability/maintainability and testability.